# Calculation of temperature distribution and rheological properties of the lithosphere along geotransect in the Red Sea region

Jana DÉREROVÁ[1], Igor KOHÚT[1], Anwar H. RADWAN[2], Miroslav BIELIK[1,3]

[1] Earth Science Institute, Slovak Academy of Sciences, Geophysical Division, Department of Gravity and Geodynamics, Dúbravská cesta 9, P.O. Box 106, 840 05 Bratislava, Slovak Republic; e-mail: geofjade@savba.sk, geofkohi@savba.sk

[2] National Research Institute of Astronomy and Geophysics, Department of Geodynamics, EL Marsad Street 1, Helwan, Cairo, Arab Republic of Egypt

[3] Department of Applied and Environmental Geophysics, Faculty of Natural Sciences, Comenius University, Mlynská dolina, Ilkovičova 6, 842 15 Bratislava, Slovak Republic; e-mail: bielik@fns.uniba.sk

**Abstract:** The temperature model of the lithosphere along profile passing through the Red Sea region has been derived using 2D integrated geophysical modelling method. Using the extrapolation of failure criteria, lithology and calculated temperature distribution, we have constructed the rheological model of the lithosphere in the area. We have calculated the strength distribution in the lithosphere and constructed the strength envelopes for both compressional and extensional regimes. The obtained results indicate that the strength steadily decreases from the Western desert through the Eastern desert towards the Red Sea where it reaches its minimum for both compressional and extensional regime. Maximum strength can be observed in the Western desert where the largest strength reaches values of about 250–300 MPa within the upper crust on the boundary between upper and lower crust. In the Eastern desert we observe slightly decreased strength with max values about 200–250 MPa within upper crust within 15 km with compression being dominant. These results suggest mostly rigid deformation in the region or Western and Eastern desert. In the Red Sea, the strength rapidly decreases to its minimum suggesting ductile processes as a result of higher temperatures.

**Key words:** the Red Sea, integrated modelling, temperature distribution, rheological parameters, strength, compression, extension, Egypt

doi: 10.1515/congeo-2017-0015 

## 1. Geological description of the study area

The oldest known formation in the Red Sea rift region (Fig. 1) is the igneous and metamorphic rocks of Late Precambrian age (*Saleh et al., 2006*). This type of rocks has been formed in the northern edge of the African Shield. In some places of the southern Sinai and in the Eastern Desert (Red Sea mountain range) the Late Precambrian basement complex outcrops. The depth of the basement increases northwards towards the Mediterranean Sea (*El-Gezeery and Marsouk, 1974*). The Palaeozoic rocks are characterized by continental clastic deposits. The marine episodes are minor in space and time. The Palaeozoic period ended with the Upper Carboniferous-Lower Permian marine deposition that followed the Hercynian orogenic phase,

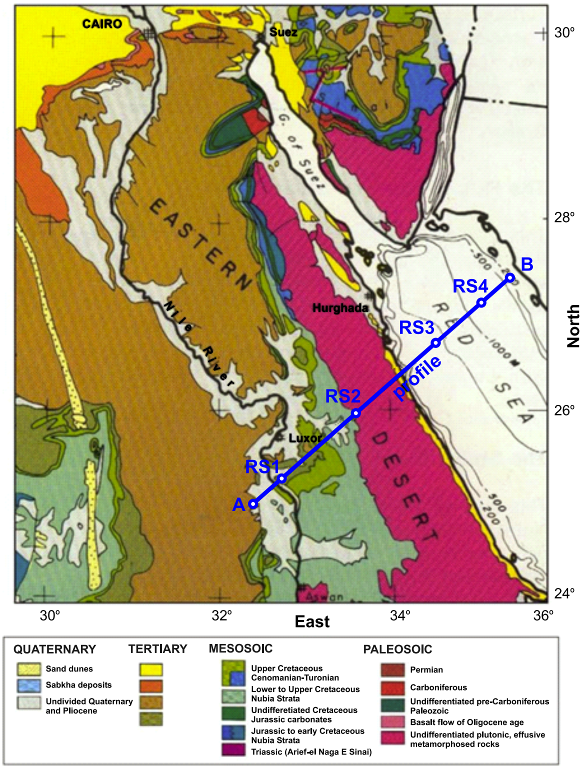


Fig. 1. Geology of the Red Sea region (*Egyptian Geological Survey, 1994*) and location of studied profile in the Red Sea region.

and the subsequent erosional period. Predominant continental deposition started again in the Mesozoic (*Saleh et al., 2006*).

Transgression of Middle Triassic marine from the Tethys appears to be limited to the area of northern Sinai and the Gulf of Suez. It is suggested that Jurassic deposits cover parts of the west side of the Gulf of Suez. It seems to be that the distribution of the Jurassic sediments around the Gulf is as far south as Wadi Araba. These sediments include fluvio-marine and marine shallow-water deposits (*El-Gezeery and Marsouk, 1974*). The maximum extension of the sea seems to have occurred during Middle Jurassic time. The Cenozoic witnessed the transformation of the Tethys into the Mediterranean Sea. During the Palaeocene–Eocene, 'deep sea conditions' migrated southwards and shallow water conditions of sedimentation or even land masses resulted in the northern part of Egypt, which now corresponds to the southern Mediterranean Sea. Thick calcareous deposits built by the Eocene limestones (the most widespread marine deposits in Egypt) are due to the deep sea evolution in the south. The limestones extend over the central part of Egypt where it constitutes a large plateau, crossed by the River Nile over a distance of 560 km, and in the central part of Sinai. The Miocene was a period of great transformation, leading to the present Red Sea coast sediments and similar sedimentation in the north-western part of the Gulf of Suez (*Saleh et al., 2006*). After the Oligocene uplift, an Early and Middle Miocene Tethys transgression began, only to be followed by late Miocene regression related to Alpine orogeny to the north. More extensive marine beds were formed in the Miocene, with a maximum extent in the Middle Miocene, when they reached to the Gulf of Suez and the Red Sea region beyond the Egyptian border. Pliocene sediments are widely distributed along the Red Sea. The Quaternary was characterized by regression with minor transgression. Uplift and tectonic disturbances mark the Pliocene-Quaternary boundary in the Red Sea region. Volcanism occurred in the Red Sea axial trough (*El-Gezeery and Marsouk, 1974; Saleh et al. 2006*).

## 2. Method

Lithospheric structure along the studied profile in the Red Sea area 1 (Fig. 1) has been previously modelled using the 2D integrated geophysical modelling approach. It is a method that combines joint interpretation of the surface heat flow, geoid, gravity, and topography data to determine the thermal structure of the lithosphere. Detailed description of method can be found in *Zeyen and Fernàndez (1994)* or *Dérerová et al. (2006).* Calculated lithospheric model for a given profile (Fig. 2) has been described in *Radwan et al. (2006).* Based on the calculated temperature field in the lithosphere, we can calculate the yield strength for a given distribution of rheological rock parameters. The strength is defined as the minimum of brittle and ductile strength at each point. For brittle strength calculation we have assumed that deformation occurs according to the frictional sliding law given by Byerlee (1978). Ductile strength is calculated assuming power-law creep deformation (*Lynch and Morgan, 1987*). Full method together with formulas can be found in *Zeyen and Fernàndez (1994)* or in *Dérerová et al. (2006).*

## 3. Results

Temperature distribution has been calculated for a given lithospheric structure model along the studied profile (Fig. 3). The lower limit of the model corresponds to 1300 °C isotherm. The temperature field is determined by the effect of the heat sources and background heat flow density from the lower mantle. The reliability of the temperature model normally depends on the accuracy and density of measurements of the surface heat flow density but since our lithological model is controlled by calculation of free air anomaly, topography and geoid, the reliability of the model increases significantly.

Based on the rheological parameters shown in Table 1a and Table 1b, the strength distribution in the lithosphere has been calculated. Fig. 4 shows vertically integrated compressional and extensional strength calculated for the studied profile. Figs. 5 and 6 show the calculated yield strength contour plot for compressional and extensional deformation. In our calculations, strain rate $10^{-15}$ s$^{-1}$ has been used, which is commonly observed in compressional and extensional settings (*Carter and Tsenn, 1987*). The strength envelopes have been calculated for both compressional and extensional regimes. Fig. 7 shows strength distribution for selected lithospheric columns (RS1–RS4) along the profile in the Red Sea region.

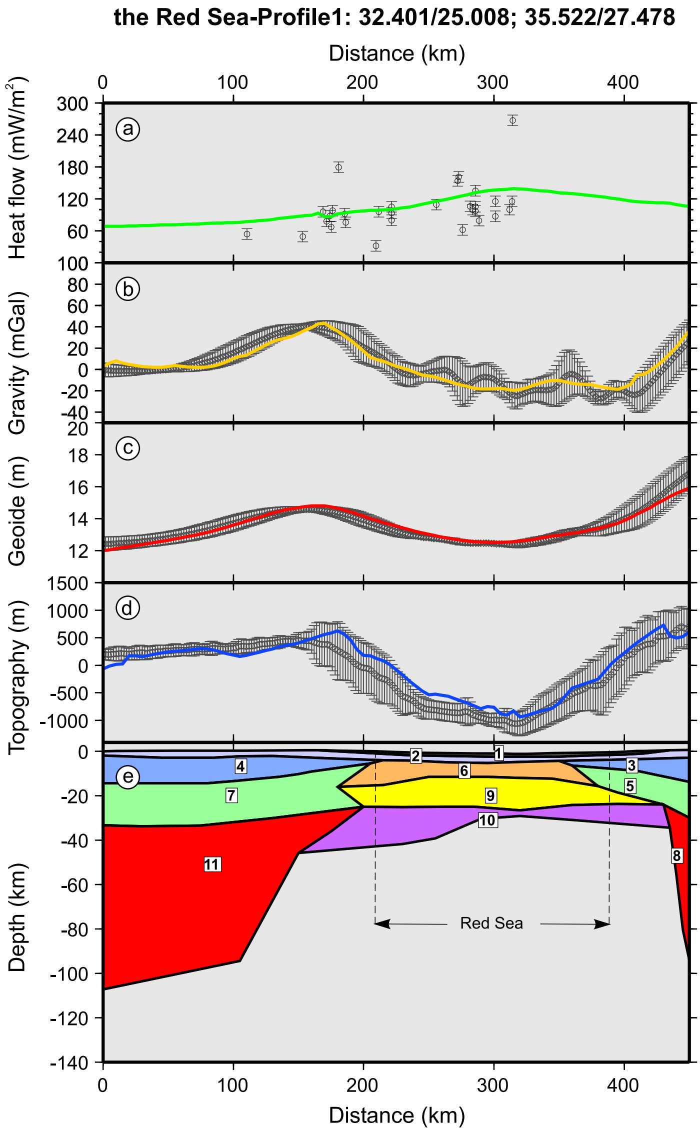


Fig. 2. Lithospheric model along profile in the Red Sea (with exact coordinates) (a) surface heat flow, (b) free-air gravity anomaly, (c) geoid, (d) topography with dots corresponding to measured data with uncertainty bars and solid lines to calculated values, (e) lithospheric structures. Numbers within the model bodies correspond to material number in Table 1b.

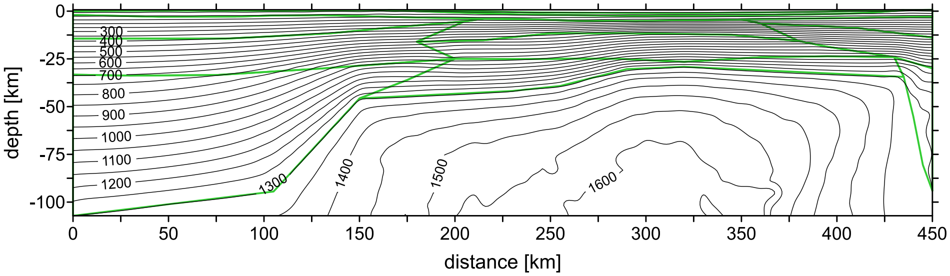


Fig. 3. Lithospheric temperature distribution for profile in the Red Sea. Isolines every 100 °C. The bottom of the model corresponds to the 1300 °C isotherm.

Table 1a. General properties used for calculation of rheological model.

| **Definition** | **Parameter** | **Value** |
|---|---|---|
| Gravity acceleration [$ms^{-2}$] | $g$ | 9.806 |
| Universal gas constant [$J mol K^{-1}$] | $R$ | 8.314 |
| Temperature at the base of the lithosphere [°C] | $T_m$ | 1300 |
| Static friction coefficient | $f_s$ | 0.6 |
| Strain rate [$s^{-1}$] | $\dot{\varepsilon}$ | $10^{-15}$ |
| Hydrostatic pore fluid factor | $\lambda$ | 0.35 |

Table 1b. Thermal and rheological parameters used for modelling along the profile in the Red Sea (after *Carter and Tsenn (1987)* and *Goetze and Evans (1979)*). HP: heat production ($\mu Wm^{-3}$), TC: thermal conductivity ($Wm^{-1}K^{-1}$), $\rho$: density at room temperature ($kg\,m^{-3}$), $A_p$: power law pre-exponential constant, $n$: power law exponent, $E_p$: power law activation energy ($kJ\,mol^{-1}$).

| **Nr.** | **Unit** | **HP** | **TC** | $\rho$ | $A_p$ | $n$ | $E_p$ |
|---|---|---|---|---|---|---|---|
| 1 | Quaternary and Pliocene sediments | 3.0 | 2.5 | 2220 | 3.16E−26 | 3.30 | 186 |
| 2 | Recent sediments | 3.0 | 2.5 | 2400 | 3.16E−26 | 3.30 | 186 |
| 3, 4 | Upper crust (basement rocks) | 2.0 | 2.0 | 2690 | 3.16E−26 | 3.30 | 186 |
| 6 | Igneous crust | 0.2 | 2.0 | 2850 | 3.16E−26 | 3.30 | 186 |
| 5, 7 | Lower crust | 0.2 | 2.0 | 2900 | 6.31E−20 | 3.05 | 276 |
| 8, 11 | Normal upper mantle | 0.05 | 3.4 | 3250 | 7.94E−18 | 4.50 | 535 |
| 9 | Red Sea upper mantle | 0.05 | 3.4 | 3200 | 7.94E−18 | 4.50 | 535 |
| 10 | Red Sea anomalous upper mantle | 0.05 | 3.4 | 3120 | 7.94E−18 | 4.50 | 535 |

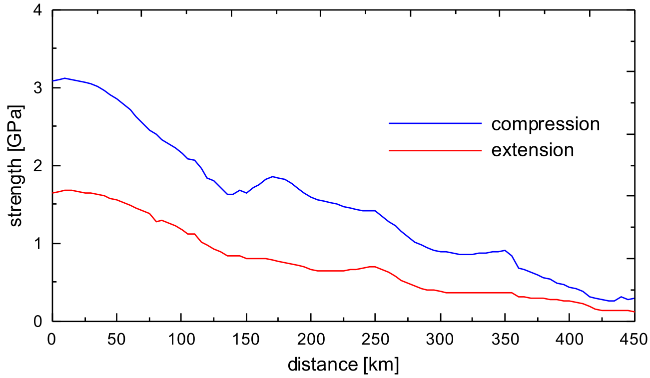


Fig. 4. Vertically integrated compressional and extensional strength calculated along the profile in the Red Sea.

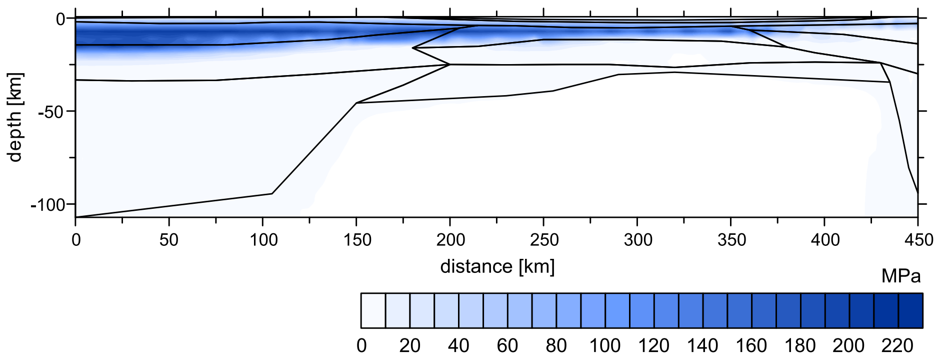


Fig. 5. Yield strength contour plot for compressional deformation calculated along profile in the Red Sea at a strain rate $10^{-15}$ s$^{-1}$.

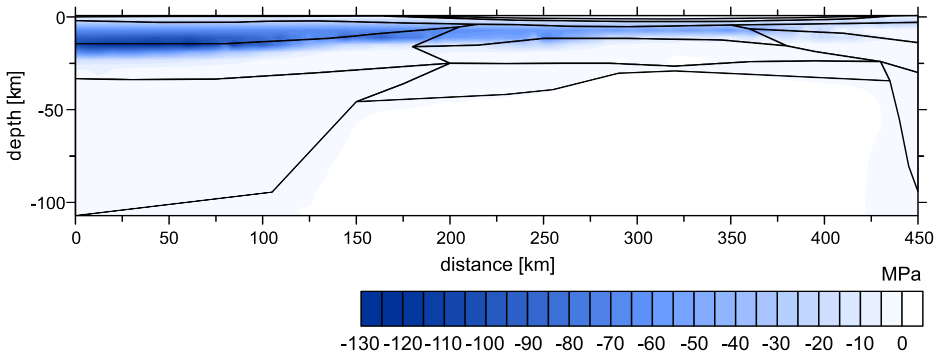


Fig. 6. Yield strength contour plot for extensional deformation calculated for along profile in the Red Sea at a strain rate $10^{-15}$ s$^{-1}$.

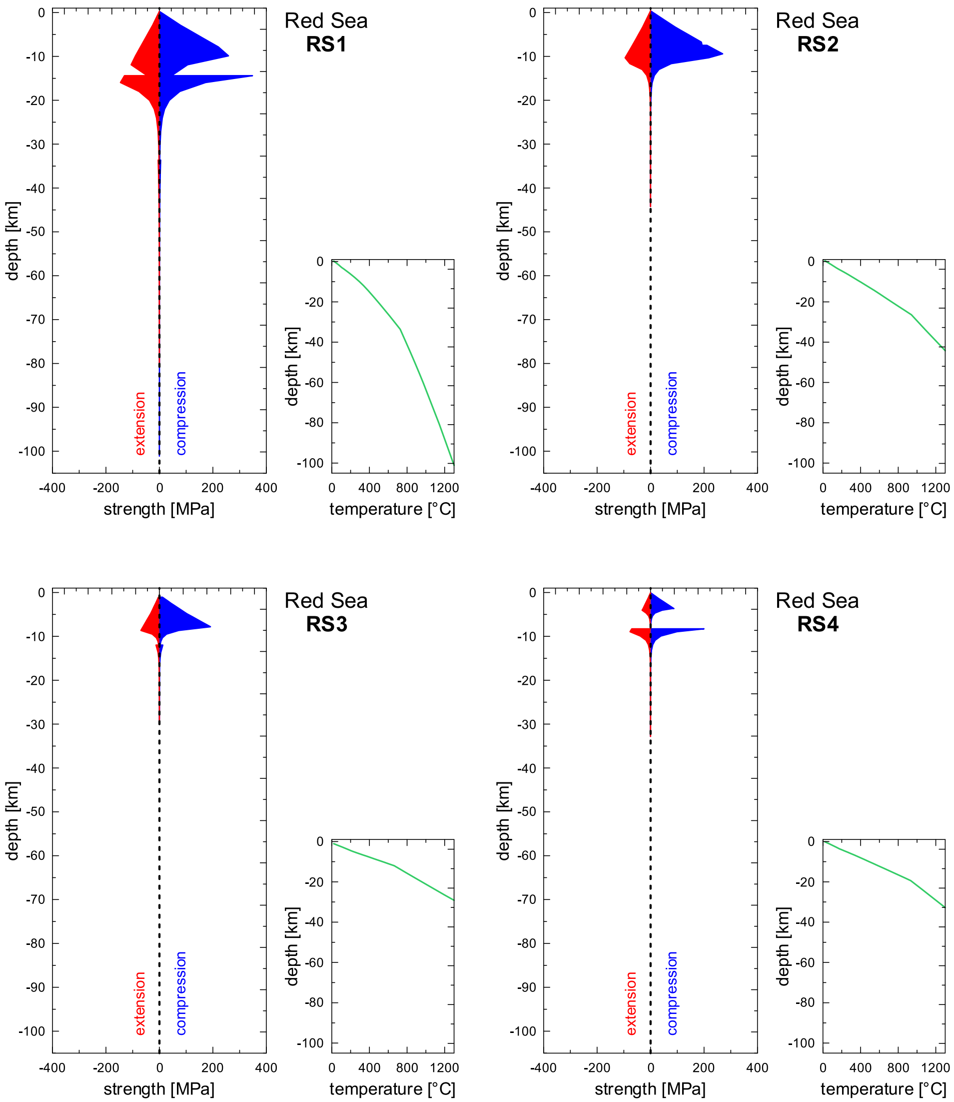


Fig. 7. Vertical strength distribution for different lithospheric columns RS1–RS4 along profile in the Red Sea. Negative and positive values correspond to extensional and compressional strength respectively.

## 4. Conclusions

2D integrated modelling approach has been used to calculate temperature and strength distribution in the lithosphere along profile that passes through the Red Sea region in Egypt. The obtained results of integrated compressional and extensional strength (Fig. 4) indicate that the strength steadily decreases from the Western desert through the Eastern desert towards the Red Sea where it reaches its minimum for both compressional and extensional regime. Calculated results for yield strength contour plot (Figs. 5 and 6) as well as for the vertical strength distribution for different lithospheric columns RS1-RS4 (Fig. 7) along profile in the Red Sea show that the maximum strength can be observed in the Western desert where the largest strength reaches values of about 250–300 MPa within the upper crust on the boundary between upper and lower crust. In the Eastern desert we observe slightly decreased strength with max values about 200–250 MPa in the upper crust within 15 km with compression being dominant. These results suggest mostly rigid deformation in the region or Western and Eastern desert. In the Red Sea, the strength rapidly decreases to its minimum suggesting ductile processes as a result of higher temperatures.

***Acknowledgements***. This research has been supported by the Slovak Grant Agency VEGA, grants No. 2/0042/15 and No. 1/0141/15, and by the Slovak Research and Development Agency under grants No. APVV-0724-11, APVV-0194-10 and APVV-0482-16. Authors are grateful to Prof. Hermann Zeyen (Laboratoires IDES, Université Paris-Sud XI) for permission to use 2D integrated modelling software.

## References

Byerlee J., 1978: Friction of rocks. Pure Appl. Geophys., **16**, 1, 615–626.

Carter N. L., Tsenn M. C., 1987: Flow properties of continental lithosphere. Tectonophysics, **136**, 27–63.

Dérerová J., Zeyen H., Bielik M., Salman K., 2006: Application of integrated geophysical modeling for determination of the continental lithospheric thermal structure in the eastern Carpathians. Tectonics, **25**, 3, TC3009, doi: 10.1029/2005TC001883.

Radwan A. H. A., Issawy E. A.-A., Dérerová J., Bielik M., Kohút I., 2006: Integrated lithospheric modelling in the Red Sea area. Contributions to Geophysics and Geodesy, **36**, 4, 373–384.

Egyptian Geological Survey, 1994: Geological map of Sinai, Arab Republic of Egypt, Scale 1:250 000.

El-Gezeery M. V., Marsouk I. M., 1974: Miocene rock stratigraphy of Egypt. Egypt. J. Geol., **18**, 1–59.

Goetze C., Evans B., 1979: Stress and temperature in the bending lithosphere as constrained by experimental rocks mechanics. Geophys. J. R. Astron. Soc., **59**, 463–478.

Lynch H. D., Morgan P., 1987: The tensile strength of the lithosphere and the localisation of extension. Continental Extension Tectonics edited by M. P. Coward, J. F. Dewey, and P. L. Hancock. Geol. Sec., Spec. Publ., London, **28**, 53–65.

Saleh S., Jahr T., Jentzsch G., Saleh A., Abou Ashour N. M., 2006: Crustal evaluation of the northern Red Sea rift and Gulf of Suez, Egypt from geophysical data: 3-dimensional modeling. Journal of African Earth Sciences, **45**, 257–278.

Zeyen H., Fernàndez M., 1994: Integrated lithospheric modeling combining thermal, gravity and local isostasy analysis: application to the NE Spanish Geotransect. J. Geophys. Res., **99**, 18089–18102.